Charge Transfer Induced Excited State Twisting of *N*,*N*-Dimethylaminobenzylidene-1,3-indandione in Solution

V. Gulbinas,*,† G. Kodis,† S. Jursenas,†,‡ L. Valkunas,† A. Gruodis,§ J.-C. Mialocq,|| S. Pommeret,|| and T. Gustavsson||

Institute of Physics, A. Gostauto 12, Vilnius 2600, Lithuania, Institute of Materials Science and Applied Research, Vilnius University, Naugarduko 24, Vilnius 2006, Lithuania, Department of General Physics and Spectroscopy, Vilnius University, Sauletekio 9, corp. 3, Vilnius 2054, Lithuania, and 4 CEA/ Saclay, DSM/DRECAM/SCM/URA331 CNRS, 91191 Gif-sur-Yvette Cedex, France

Received: November 30, 1998; In Final Form: March 3, 1999

Nonradiative excited-state relaxation via charge transfer induced twisting of *N*,*N*-dimethylaminobenzylidene-1,3-indandione (DMABI) in solution was investigated by means of picosecond transient absorption and femtosecond fluorescence spectroscopy.The analysis of the experimental data allows us to distinguish between different reaction stages of the molecular twisting in excited and ground states, as well as to consider the molecular dynamics along reactive (twisting) and nonreactive (solvation) coordinates. Quantum chemical calculations of the electronic structure of DMABI and its dependence on the molecular conformation are discussed in order to identify the bond(s) involved in the twisting reaction. It is found that such a twisting bond is the C═C double bond, which is substantially weakened in the excited state.

Introduction

Understanding of the fundamental processes responsible for the ultrafast nonradiative excited-state relaxation so often observed in organic charge-transfer molecules in solution is a very important issue in contemporary molecular photochemistry. It is today well-known that intramolecular charge separation[1−16] and photoisomerization[1−5,17−32] constitute two different aspects of this problem. For the majority of simple organic molecules containing the electron-donating and -accepting parts, the charge separation is more favorable in a twisted conformation, where the two moieties involved in the charge transfer are orbitally decoupled; i.e., they are positioned in the nearly perpendicular planes. The mechanism of the charge transfer and twisting motion is, however, difficult to describe precisely.

A coupling of the charge transfer and the twisting reactions was first suggested by Rotkiewicz, Grellmann, and Grabowski in 1973 in order to describe the dynamical relaxation of a simple benzene derivative, namely, *p*-*N*,*N*-dimethylaminobenzonitrile (DMABN).[33] The notions of "locally excited" (LE) and "twisted intramolecular charge transfer" (TICT) states[33−63] were evoked to describe the dual fluorescence observed.[64] It has been understood that in many cases TICT states are nonluminescent, creating a rapid nonradiative decay channel and, consequently, are responsible for fluorescence quenching.

Several models have been proposed to explain the solvent influence on charge transfer and isomerization reactions. The Sumi and Marcus (SM) theory[7] for electron transfer and the Bagchi, Fleming, and Oxtoby (BFO) theory[18] for barrierless isomerization reactions are the most intensively used among them. According to SM theory, the electron position during the intramolecular electron-transfer reaction is determined by the solvation shell. Thus, a generalized solvation coordinate is involved in describing the time course of the reaction. In the case of isomerization dynamics, the BFO theory uses the twisting angle as the reaction coordinate. In the TICT model both the intramolecular twisting motion and solvation dynamics are considered as friction-affected and being of a similar rate, but most importantly, the two processes are supposed to be coupled.

Bagchi and Fleming[2] used a two-dimensional Smoluchowski equation to describe the barrierless reaction dynamics in solution. Recently, this formalism has been used by Kim and Hynes[53] to calculate the reaction path of the TICT process in DMABN on a two-dimensional surface. The reaction dynamics and properties of the TICT states depend on the reactant molecular structure, the solvent parameters, and the solute−solvent interaction. However, these dependences even for the most intensively studied DMABN molecule are not completely clear yet, while the relation of the reaction properties with the molecular structure is still very vague.

Results of the investigation of the photoinduced charge transfer and twisting reaction of *N*,*N*-dimethylaminobenzylidene-1,3-indandione (DMABI) in solution as well as in a polymeric matrix are presented in this paper. To the best of our knowledge, the twisting reaction of the molecule containing the highly electron-accepting 1,3-indandione group has not been considered so far. The reaction dynamics was examined by means of picosecond transient absorption and femtosecond fluorescence measurements. Both these time-resolved methods together with quantum chemical calculations usefully supplemented each other, enabling us to distinguish different reaction stages in singlet excited and ground states and to study their dynamics along the twisting and solvation coordinates.

DMABI Structure and Quantum Chemical Calculations. *N*,*N*-Dimethylaminobenzylidene-1,3-indandione (DMABI) (Figure 1) belongs to the polar derivatives of 1,3-indandione. It

* To whom correspondence should be addressed. E-mail: vidgulb@ktl.mii.lt.
† Institute of Physics.
‡ Institute of Materials Science and Applied Research, Vilnius University.
§ Department of General Physics and Spectroscopy, Vilnius University.
|| 4 CEA/ Saclay.

10.1021/jp9845468 CCC: $18.00
Published on Web 04/29/1999

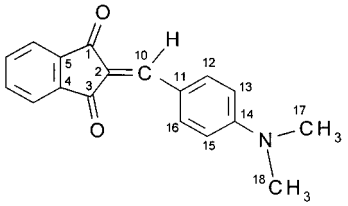

Figure 1. Structural formula of the DMABI molecule.

consists of two chromophores, 1,3-indandione and dimethylaminophenyl, connected via a methyne (=CH−) bridge. Owing to the electron-donor and electron-acceptor properties of the different fragments, an intramolecular charge transfer takes place, resulting in an asymmetrical charge distribution and, consequently, in large dipole moments in both the ground and excited states. The dipolar character of DMABI has been already discussed in several pioneering studies since the early 1970s.[65] The structure of DMABI was examined by Magomedova et al.[66] who performed a detailed X-ray analysis of the DMABI crystals and revealed that the DMABI molecule in the crystal is practically flat (dihedral angles $\varphi_1(C_1-C_2=C_{10}-C_{11}) = 4.3°$, $\varphi_2(C_2=C_{10}-C_{11}-C_{12}) = 0°$, and $\varphi_3(C_{13}-C_{14}-N-C_{18}) = 0°$) and that the long axes of the donor and acceptor fragments form an angle $\omega_1(C_2=C_{10}-C_{11}) = 134.6°$. Semiempirical quantum chemical calculations of DMABI also predicted the predominant molecular configuration to be flat,[67] and values of static dipole moments in the ground and excited states ($d_{gr} = 2.3$ D, $d_{ex} = 14.22$ D) were obtained.

Here, additional semiempirical and ab initio quantum chemical calculations are undertaken in order to relate optical properties of the molecule with its electronic structure and to determine the influence of the molecular conformation on the energy spectrum and the transition dipole moments. Investigations of molecular states were carried out by means of the MO CNDO/S (complete neglect of differential overlap − for spectra) method in the Mataga−Nishimoto approximation.[68] The electronic ground-state conformation of the DMABI molecule was optimized using the ab initio Gaussian-94 program[69] in the B3LYP/6-311G* basis set.[70]

According to the ab initio optimization procedure, the minimum of the ground-state energy corresponds to the following conformation with bond lengths (see Figure 1) $d_1(C_2=C_{10}) = 1.371$ Å, $d_2(C_{10}-C_{11}) = 1.436$ Å, and $d_3(C_{14}-N) = 1.379$ Å, bond angles $\omega_1(C_2=C_{10}-C_{11}) = 134.6°$, $\omega_2(C_{10}-C_{11}-C_{16}) = 125.6°$, $\omega_3(C_{10}=C_2-C_1) = 119.0°$, and dihedral angles $\varphi_1(C_1-C_2=C_{10}-C_{11}) = -0.0006°$, $\varphi_2(C_2=C_{10}-C_{11}-C_{12}) = 0.014°$, and $\varphi_3(C_{13}-C_{14}-N-C_{18}) = 0.051°$.

The three lowest excited states of the DMABI molecule are close to each other. The two lowest S_1 and S_2 states are of $n\pi^*$ type; therefore, transitions $S_0 \rightarrow S_1$ and $S_0 \rightarrow S_2$ are optically forbidden, since the calculated oscillator strengths are equal to 0.0009 and 0.0003, respectively. The S_3 state is of $\pi\pi^*$ type and is responsible for the lowest optically allowed transition $S_0 \rightarrow S_3$ with oscillator strength 0.7557. This transition corresponds to the visible absorption band; however, the transition energy obtained from calculations equals 3.73 eV, which is significantly higher than the experimentally obtained value (2.71 eV in heptane). It should be noted that many organic molecules containing heteroatoms have a similar electronic structure. For example, acroleinimine[71] is also characterized by the two lowest S_1 and S_2 excited states of $n\pi^*$ type and S_3 of $\pi\pi^*$ type.

The free energy of the molecule both in the ground and excited states has been calculated as a function of dihedral angles φ_1, φ_2, and φ_3. The excited-state free energy of the twisted molecule cannot be obtained directly by the CNDO/S method. Therefore, the ground-state free energy and energies of the three optical transitions were calculated for various molecular geometric configurations, and consequently, free energies of the excited states were evaluated from these data. The calculations showed that twisting of both single bonds of the molecule by changing angles φ_2 and φ_3 resulted in a monotonic energy increase in the ground state and in all three excited states, indicating that such twisting is not energetically favorable and therefore does not occur. This is because electronic charge redistribution takes place after excitation, making the charge density on the single bonds higher than that on the double bond. The calculated free energy dependence on the double bond twisting angle φ_1 is presented in Figure 2a. The S_1 excited state has an energy minimum at the 90° twisting angle, and the S_3 state has a local minimum at ca. 50°.

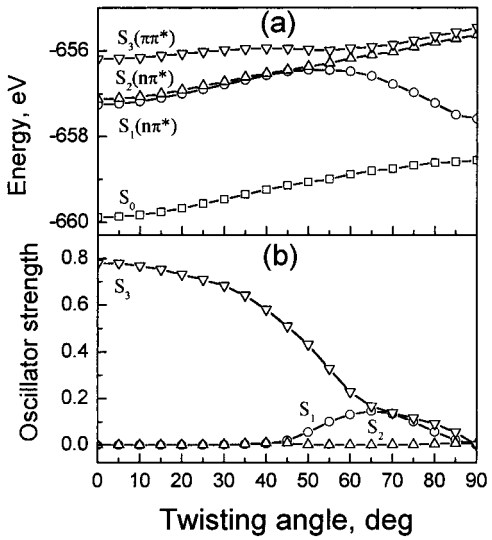

Figure 2. Energy (a) and oscillator strengths (b) of the ground-state S_0 and three lowest excited singlet states S_1, S_2, and S_3 as a function of the dihedral angle φ_1.

Figure 2b shows oscillator strengths of the three optical transitions as a function of the twisting angle. The oscillator strength of the $S_0 \rightarrow S_3$ transition is maximal at 0° and decreases with increasing twisting angle, becoming optically forbidden at 90° because of the different symmetry of the ground and the excited states. However, the $S_0 \rightarrow S_1$ transition gains oscillator strength at larger twisting angles.

The calculated properties of the DMABI molecule indicate the possibility of the double bond twisting in the excited state. However, the calculated energy scheme should be accepted only as a tentative one. The solvent effect was not taken into account, and the calculation did not allow for energy minimization by changing the reaction coordinate. Therefore, significant error could occur, particularly at large twisting angles, since changes in other molecular parameters were not taken into account.

Experimental Section

DMABI (*N*,*N*-dimethylaminobenzylidene-1,3-indandione) was synthesized and purified by gradient sublimation techniques at the Institute of Physical Energetic in Riga as described in ref 72. All solvents used for preparation of the DMABI solutions were reagent grade and used without additional purification. A polymeric film of DMABI was prepared by dissolving polyvinylbutyral in an ethanol−butanol mixture and then adding some DMABI−EtOH solution. The solution was finally poured on a glass substrate and left to dry.

Absorption spectra were measured with a spectrophotometer (Beckman UV 5270). Steady-state fluorescence spectra were obtained under CW Ar^+ laser excitation at 488.0 nm by using a photomultiplier operating in the photon-counting regime and a double grating monochromator DFS 52 (Soviet production). This setup was also used to determine the fluorescence quantum yields and their dependence on solvent viscosity.

Femtosecond time-resolved emission spectra and their kinetics were obtained by the fluorescence upconversion technique. The experimental setup has already been described.[73] The femtosecond laser source was a Ti:sapphire laser (Coherent MIRA 900) pumped by a CW Ar^+ laser (Coherent IRA 900) generating light pulse of 125 fs fwhm. The samples were excited at 394 nm by the second harmonic of the laser radiation. After passage through a delay-line, the residual fundamental was focused into a 0.2 mm BBO upconversion crystal, thus serving as the gating pulse for sum-frequency generation. The fluorescence was collected with a parabolic mirror and focused into the upconversion crystal together with the gating pulse. The upconverted light was focused onto the entrance slit of a monochromator (Jobin-Yvon HR250), and the spectrally selected upconversion light was detected by a photomultiplier connected to a lock-in photon counter. Time-resolved fluorescence spectra were recorded directly by simultaneously changing the monochromator wavelength, rotating the upconversion crystal, and changing the delay-line position in order to compensate the group velocity dispersion. The fluorescence kinetics was measured by changing only the delay-line position. The experimental time resolution was better than 100 fs.

The picosecond transient absorption study was performed by using a pump−probe spectrometer based on a homemade low repetition rate Nd:glass laser delivering pulses of 2 ps duration. The second harmonic of the fundamental light (527 nm) was used for excitation, and a white-light continuum was generated in a water cell to probe the samples. The continuum was split into two parts that passed through the sample at different positions, one overlapping with the excitation pulse, the second a few millimeters beside the first, serving as the reference. Both pulses were focused onto the monochromator entrance slit, and their energies at selected wavelengths were measured using photodiodes positioned behind the exit slit. Transient absorption kinetics at a selected wavelength was measured by changing the delay time between the excitation and the probe pulses. Transient absorption spectra at a fixed delay time were recorded by changing the monochromator wavelength and simultaneously changing the delay-line in order to compensate the group velocity dispersion.

Experimental Results

Steady-State Absorption and Fluorescence Spectra. The fluorescence quantum yield of the DMABI solutions is very low. It is lower than 1% in low viscosity solvents (0.25% in ethanol) while increasing (approximately) proportionally to the solvent viscosity in different alcohols. A very significant increase in the fluorescence yield is observed in a polymeric matrix. The fluorescence quantum yield decreases with increasing temperature; however, owing to a strong correlation between the fluorescence yield and the solvent viscosity, this temperature dependence can be attributed to variation of the viscosity. No correlation between the fluorescence quantum yield and the solvent polarity was obtained.

The steady-state absorption and fluorescence spectra of DMABI solutions in hexane, in dimethyl sulfoxide (DMSO), and in a polymeric polyvinylbutyral (PVB) film are shown in Figure 3. In the nonpolar hexane the absorption spectrum has a well-expressed shoulder on the short-wavelength side of the band, which may be attributed to vibronic structure. In polar DMSO, as well as in the polymeric film, the solute−solvent interactions are more pronounced, resulting in broader absorption spectra and the disappearance of the vibronic structure. Figure 4 shows the dependence of the absorption and fluorescence maximum positions on the empirical polarity parameter π^* [74−79] and the solvent reaction field factor F defined as[75]

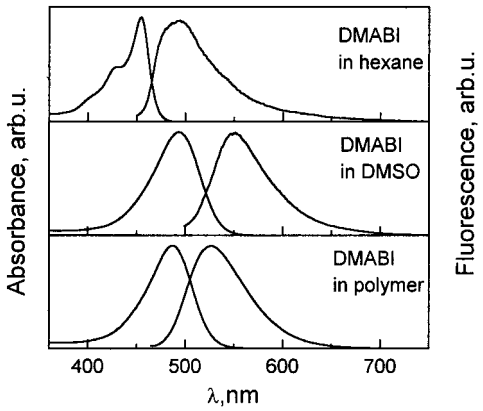

Figure 3. Absorption and fluorescence spectra of the DMABI in hexane, in dimethyl sulfoxide (DMSO), and in polymeric polyvinylbutyral (PVB) film.

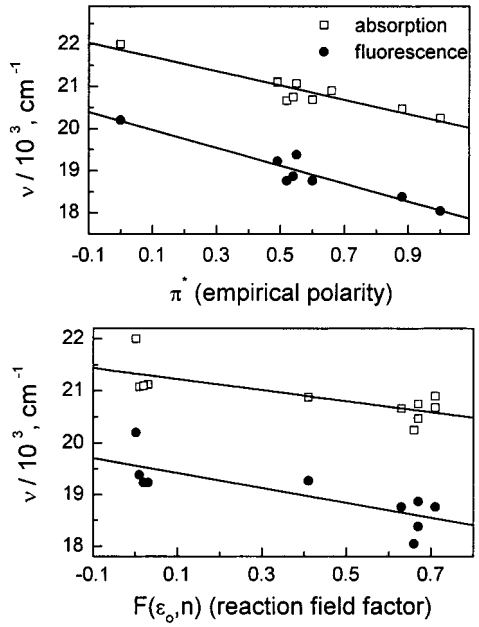

Figure 4. Absorption and fluorescence peak frequencies vs solvent polarity and reaction field factor.

$$F(\epsilon_0,n) = \frac{\epsilon_0 - 1}{\epsilon_0 + 2} - \frac{n^2 - 1}{n^2 + 1} \qquad (1)$$

where ϵ_0 is the static dielectric constant and n is the optical refractive index of the solvent. The correlation with the reaction field factor F is poor, while the correlation with the empirical polarity parameter π^* is quite good. No correlation between the spectral positions and the refractive index is obtained (not shown). Both the absorption and fluorescence spectra positions are defined by the first term of eq 1, which results from the solvation energy due to the nuclear polarizability. However, peculiarities of the fluorescence spectra and their dependence on solvent parameters cannot be explained only by solvation. For example, the fluorescence spectrum in hexane is even

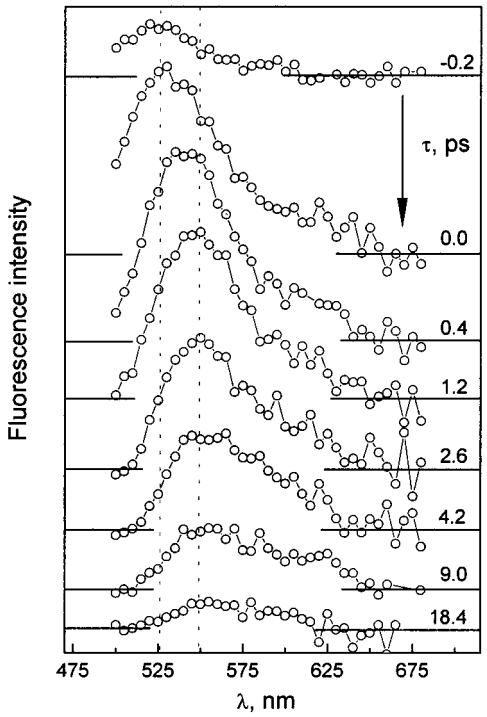

Figure 5. Time-resolved fluorescence spectra of DMABI in DMSO.

broader than that in polar solvents. The fluorescence spectra of the solutions also have very long tails on the red side of the band, particularly in hexane.

Time-Resolved Fluorescence. Time-resolved fluorescence spectra and their intensity kinetics were studied for DMABI solutions in heptane, toluene, ethanol, and DMSO. As an example, the time evolution of the fluorescence spectrum of DMABI in DMSO is shown in Figure 5. One can observe a fast fluorescence band shift toward long wavelengths accompanied by rapid intensity decay. The shoulder of the fluorescence band on the long-wavelength side appears with subpicosecond time delay and decays slightly more slowly than the main band. Qualitatively, similar spectral dynamics was also obtained in other solvents (not shown). To characterize the spectral evolution, each time-resolved spectrum was converted into the frequency scale by λ^2 rescaling and fitted by a simplified log-normal function:

$$\epsilon(\nu) = \epsilon_0 \exp\left[-\beta^2\left(\ln\frac{\nu - a}{b}\right)^2\right] \quad (2)$$

where ϵ_0, β, a, and b were the fitting parameters. This function allows calculation of the integral fluorescence intensity, the mean frequency ν_{mean}, fwhm, and asymmetry ρ as

$$\nu_{mean} = a + b\exp\left(\frac{3}{4\beta^2}\right) \quad (3)$$

$$\text{fwhm} = 2b\sinh\left(\frac{\sqrt{\ln 2}}{\beta}\right) \quad (4)$$

$$\rho = \exp\left(\frac{\sqrt{\ln 2}}{\beta}\right) \quad (5)$$

The spectral asymmetry and width showed no well-expressed time dependence. Therefore, to obtain higher accuracy of the mean frequency and the integral intensity, only ϵ_0 and a were varied during the second approach of fitting, while β and b were kept constant, equal to mean values obtained during the first

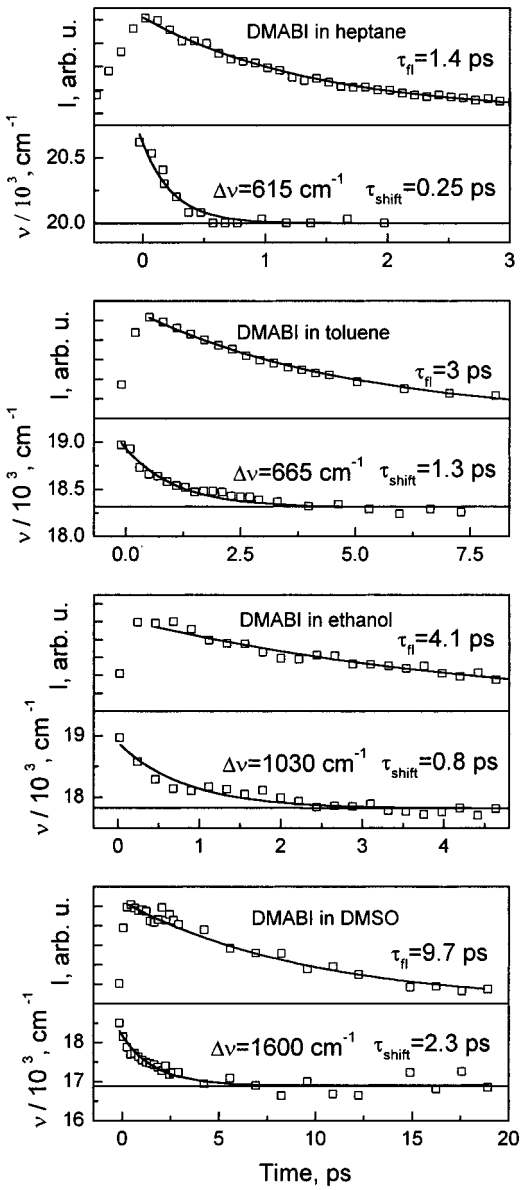

Figure 6. Integral fluorescence intensity (I) and peak frequency (ν) dynamics of DMABI in heptane, toluene, ethanol, and DMSO.

TABLE 1: Fluorescence Relaxation τ_{fl} and Dynamic Shift τ_{shift} Times and the Shift Values $\Delta\nu$ of DMABI in Various Solvents

solvent	heptane	toluene	ethanol	DMSO
τ_{fl}, ps	1.4	3	4.1	9.7
τ_{shift}, ps	0.25	1.3	0.8	2.3
$\Delta\nu$, cm^{-1}	615	665	1030	1060

turn of fitting. The integral fluorescence intensity and the mean frequency of DMABI in different solvents obtained by such a fitting are presented in Figure 6. To evaluate the time dependence of these two observables, they were fitted by a single exponential. Characteristic times of the total intensity decay and of the dynamic Stokes shift are given in Table 1. The fluorescence decay is well approximated by a single exponential in all solvents, but approximation of the Stokes shift dynamics is rough, since peak frequencies at long times cannot be well defined because of the short excited-state lifetime.

To achieve better accuracy of the fluorescence decay dynamics, measurements at fixed wavelengths close to the steady-state fluorescence maxima were also undertaken. These measurements were performed with parallel and perpendicular

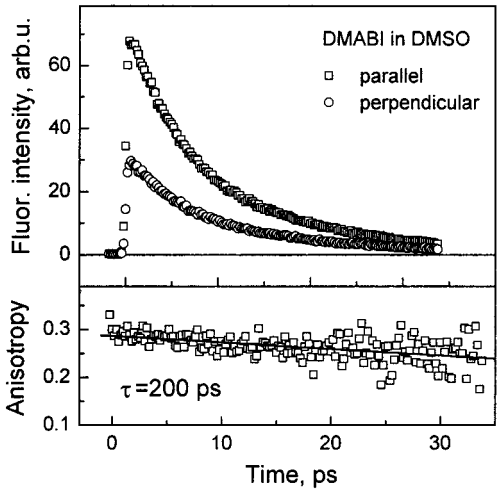

Figure 7. Fluorescence decay dynamics at 555 nm of DMABI in DMSO measured at 0° and 90° with respect to the excitation polarization and the fluorescence anisotropy decay calculated from these curves.

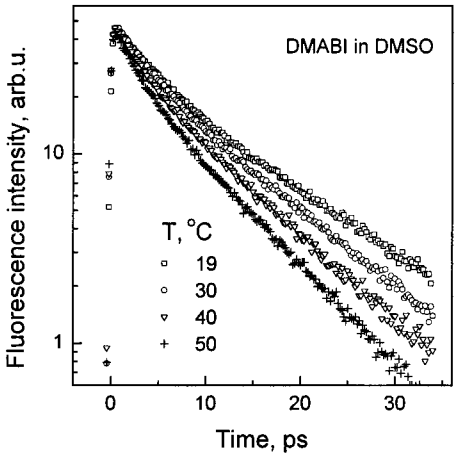

Figure 8. Fluorescence decays at 555 nm of DMABI in DMSO at various temperatures.

excitation and detection polarizations for determination of the fluorescence anisotropy dynamics as well. The results for DMABI in DMSO are shown in Figure 7. The major part of the fluorescence relaxation is well described by an exponential with a time constant close to that determined from the spectral dynamics. However, owing to the better accuracy, an additional slow decay component of small amplitude was also defined. The initial value of the fluorescence anisotropy is equal to ca. 0.3 for all solvents, which is slightly less than the maximal theoretical value (0.4) corresponding to the same orientations of the absorption and emission dipole moments. The slow anisotropy decay can be attributed to rotational diffusion of the DMABI molecules, giving a decay constant for the DMSO solution of ca. 200 ps.

The effect of temperature on the fluorescence decay of DMABI in DMSO is shown in Figure 8. Since the measurements were performed on the short-wavelength side of the fluorescence spectrum at 540 nm, biexponential kinetics was obtained. The fast decay component is evidently related to the fluorescence shift, and the slower one reflects the integrated intensity decay. Similar measurements were also performed for the methanol solution (not shown). Results of the biexponential fitting of the kinetics are summarized in Figure 9, where the dependence of both time constants on the ratio of the solvent viscosity and temperature is presented. Linear behavior, typical of the diffusion-controlled processes, indicates that rates of both

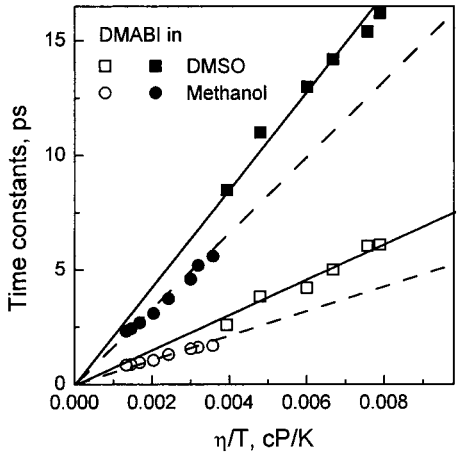

Figure 9. Fluorescence decay time constants of DMABI in DMSO (squares) and methanol (rings) at different temperatures as a function of the solvent viscosity. The time constants were obtained from biexponential fits: open symbols, τ_1; solid symbols, τ_2.

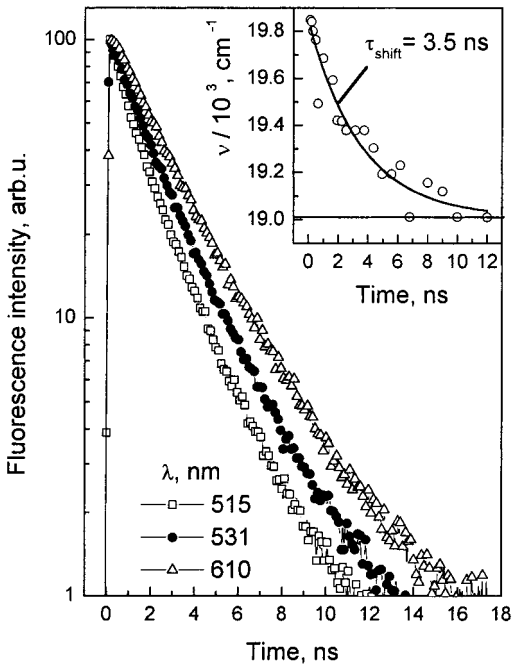

Figure 10. Fluorescence decays at different wavelengths of DMABI in a polyvinylbutyral matrix. The inset shows the fluorescence peak frequency dynamics evaluated from the decays.

the dynamic fluorescence shift and the fluorescence intensity decay are defined by the solvent viscosity. However, the slopes of the dependence plots are slightly different for different solvents, indicating that processes at the same viscosity are slightly slower in the DMSO solution.

The fluorescence decay dynamics of DMABI dispersed in a polymeric polyvinylbutyral matrix is shown in Figure 10. Measurements were performed by the gated single photon counting method on the blue side, on the red side, and in the central part of the fluorescence band. Fluorescence lifetimes and consequently the fluorescence quantum yield increase significantly in the polymer in comparison with those in solutions. The fluorescence decay is nonexponential and wavelength-dependent. The initial part of the decay measured in the central part of the band can be well characterized by the 2−2.5 ns time constant, while the decay rate decreases several times after 10 ns. The decay is slower at longer wavelengths. Such wavelength dependence can be a consequence of the dynamical shift of the

fluorescence band toward the red side. By assuming that the fluorescence band shape does not vary in time, the band shift dynamics may be determined from the time dependence of the intensity ratio at three spectral points. The calculated time-dependent spectral shift of the fluorescence band is shown in the inset of Figure 10. The shift value is about 840 cm^{-1}, which is close to the value observed in the toluene solution, and in a single-exponential approximation a 3.5 ns time constant is obtained. Similar to the behavior in solutions, this spectral shift may be attributed to environment relaxation, but it may also be explained by the heterogeneity of the system and consequently by spectral diffusion. Variations of the excited-state lifetimes and of the fluorescence spectra result from different molecular conformations and/or different environments. Different lifetimes result in nonexponential fluorescence decays and the spectral shift reflects the energy migration toward molecules having lower excited-state energy. Additional investigations, for example, the temperature dependence, may give the answer as to what extent one or the other of the two processes dominates.

Transient Absorption. Studies of DMABI solutions in methanol, propanol, decanol, DMSO, and benzonitrile and in the polymer matrix were also carried out by means of picosecond transient absorption spectroscopy. Molecules in nonpolar solvents were not convenient for such investigations, since the absorption spectra are shifted too far to the blue for efficient excitation at 527 nm. The transient absorption spectrum of DMABI in DMSO measured at various delay times after excitation is shown in Figure 11. The transient absorption spectrum changes significantly when increasing the probing delay time. To obtain a better understanding of the changes taking place, the transient absorption spectra were deconvoluted into the ground-state absorption bleaching $S_{ab}(\nu)$, stimulated emission $S_{se}(\nu)$, and the induced excited-state absorption $S_{ia}(\nu)$ components:

$$\Delta A(\nu) = -S_{ab}(\nu) - S_{se}(\nu) + S_{ia}(\nu) \tag{6}$$

The band shape of the absorption bleaching is assumed to resemble the band shape of the ground-state absorption spectrum (this assumption is valid for solutions when the inhomogeneous broadening is small and/or has a dynamic character). Stimulated emission spectra at different delay times were obtained from the time-resolved fluorescence spectra $\Phi^t(\nu)$ (see the preceding paragraph) at corresponding delay times:

$$S_{se}^t \propto \frac{\Phi^t(\nu)c^3}{8\pi h n^2 \nu^4} \tag{7}$$

where c and n are the velocity of light and the refractive index, respectively. The stimulated emission spectra thus calculated were normalized to the long-wavelength part of the transient absorption spectra by assuming that excited-state absorption is absent or weak in this spectral region. The ground-state absorption spectrum was normalized to the transient absorption spectrum at the maximum of the bleaching band. The induced absorption spectrum was then calculated according to eq 6.

The deconvolution shows that at very early times, i.e., at −2 ps, when the probe pulse slightly precedes the excitation pulse, and at 0 ps, the contributions to the transient absorption spectrum from the ground-state absorption bleaching and the stimulated emission are of similar importance, indicating that the oscillator strength of the stimulated emission is approximately equal to that of the ground state absorption. When the delay time is increased, the stimulated emission spectrum shifts to the red and its intensity decreases faster than that of the ground-state

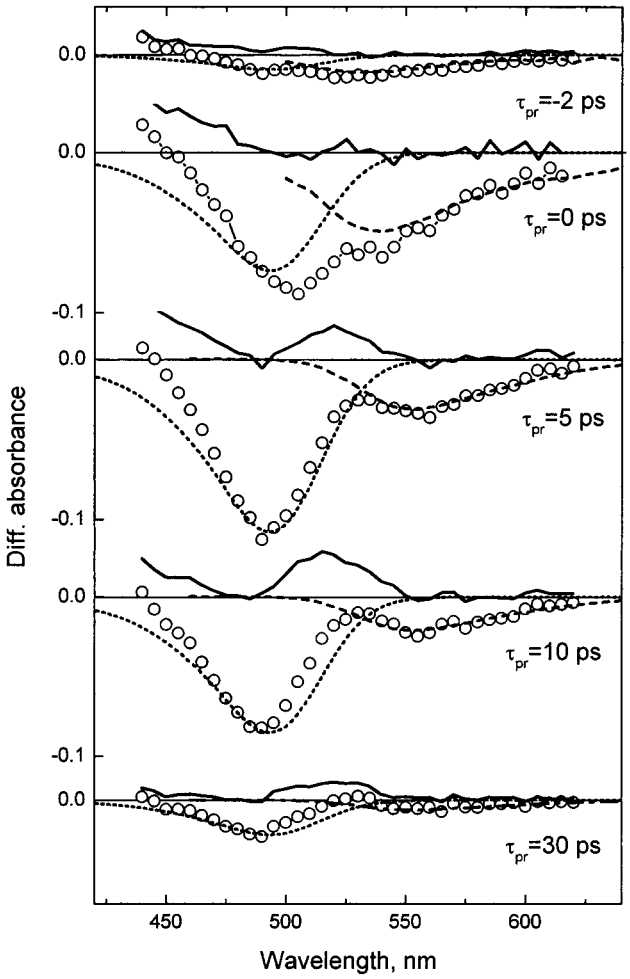

Figure 11. Transient difference absorption spectra of the DMABI in DMSO measured at various delay times after excitation. Lines show deconvolution of the spectra into absorption bleaching (dotted), stimulated emission (dashed), and induced absorption (solid) components.

absorption bleaching. This may be interpreted either as a decrease in the emission oscillator strength due to a change in the excited-state electronic structure or as a decrease in the population of emitting species due to transfer into nonemitting excited states. The induced absorption spectrum also changes very significantly in time. At short delay times the induced absorption (IA) is dominated by a band on the blue side of the spectrum (blue IA band around 440 nm). When the delay time increases, a new induced absorption band appears between the ground-state absorption bleaching and the stimulated emission bands (green IA band around 530 nm). The blue IA band may be attributed to absorption of the excited Franck−Condon state, while the green IA band belongs to some product state, a fact corroborated by its different time dependence.

A slight evolution in the blue part of the absorption-bleaching band can be explained by solvation in the ground state. The blue part of the inhomogeneously broadened absorption spectrum (due to the dynamical nonuniform solvation) is not bleached initially after excitation on the red edge of the DMABI absorption band. Bleaching of the entire absorption band arises in the course of the solvation when the equilibration of the initially created nonequilibrium ground-state depletion takes place.

The dynamics of the transient absorption is more clearly shown in Figure 12, where the absorption kinetics for DMABI in DMSO at different wavelengths is presented. Fitting curves of the kinetics approximated by one or three exponentials are also shown. The fitting procedure reveals four main relaxation

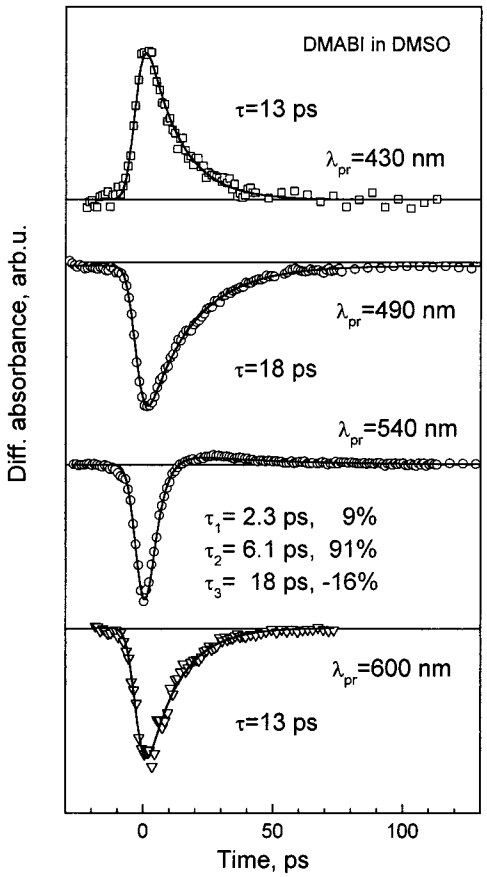

Figure 12. Transient absorption kinetics of DMABI in DMSO at different wavelengths.

times. The shortest one, the 2 ps component observed on the blue side of the stimulated emission band, is evidently due to the solvation-induced emission band shift, since this time constant is close to the dynamic fluorescence shift time. A longer component of 13 ps characterizes the decay of the blue IA band and the decay of the long wavelength part of the stimulated emission band. This component should be related to the relaxation of the excited state. The absorption bleaching decays with an 18 ps time constant. A similar relaxation time was observed in the decay of the green IA band at 535 nm, which, however, appears with a 6.1 ps delay.

The transient absorption spectra of DMABI in other solvents are qualitatively similar. The corresponding spectral changes in benzonitrile are presented in Figure 13. The fluorescence spectral dynamics was not measured in this solvent; therefore, the deconvolution procedure described above could not be applied. There is no substantial difference between the transient absorption spectra of DMABI in solvents of different polarity. In solvents of lower polarity the spectra are just shifted to shorter wavelengths. More important spectral changes are obtained by changing the solvent viscosity. All processes become faster in solvents of lower viscosity, and the intensity of the green IA band increases significantly. In benzonitrile, for example, the induced absorption at 30 ps delay time is even close to that of the ground-state absorption bleaching. This viscosity dependence is clearly seen in Figure 14 where relaxation kinetics at 490 and 540 nm of DMABI solutions in various alcohols is presented. The induced absorption is very strong in methanol and is absent in decanol. Relaxation times of the four relaxation processes (three if the green IA is absent) are summarized in Table 2. These relaxation times correlate well with the solvent viscosity, and the sequence of increasing relaxation times for

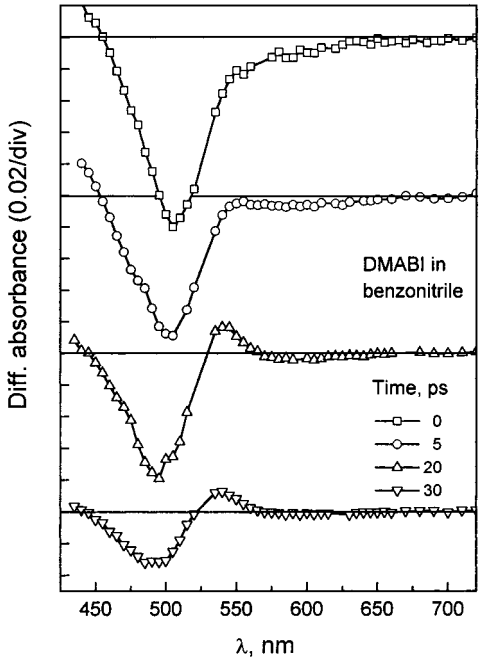

Figure 13. Transient difference absorption spectra of the DMABI in benzonitrile measured at various delay times after excitation.

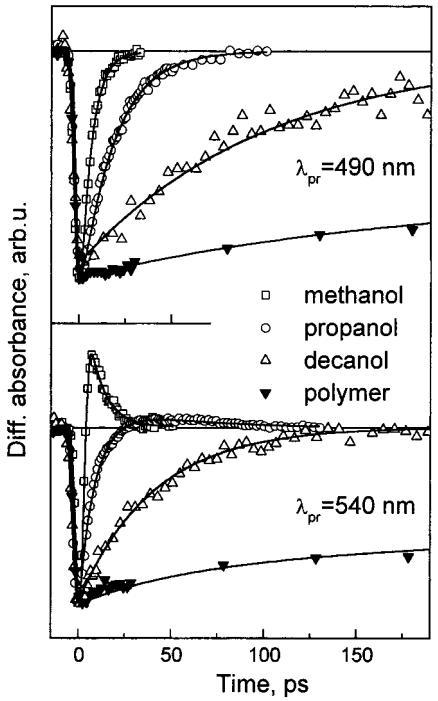

Figure 14. Relaxation kinetics at 490 and 540 nm of DMABI in various alcohols and in a polymeric matrix.

the different processes, as observed in DMSO, remains qualitatively the same.

The transient absorption spectrum of DMABI in a polymer matrix (not shown) is less complex. It only shows an induced absorption in the blue spectral region and the negative transient absorption corresponding to the sum of the ground-state absorption bleaching and stimulated emission. No substantial dynamics of the spectral shape is observed; only a slight decay of the entire spectrum takes place in 1 ns.

Discussion

The low fluorescence quantum yield and very short excited-state lifetime of the DMABI molecule in solution are direct indi-

TABLE 2: Relaxation Times of DMABI in Various Solvents at Different Probe Wavelengths[a]

	$\lambda_{pr} = 440$ nm	$\lambda_{pr} = 490$ nm	$\lambda_{pr} = 540$ nm			$\lambda_{pr} = 600$ nm
solvent	τ_{440}, ps	τ_{490}, ps	τ^1_{540}, ps	τ^2_{540}, ps	τ^3_{540}, ps	τ_{600}, ps
methanol	≤2	5.9		2.6 (−100%)	5.9 (45%)	≤2
propanol	11	18.1	2 (−10%)	9.8 (−90%)	18.1 (31%)	13
decanol	7 (40%)[b] 56 (60%)	100		40		17 (−13%)[b] 60 (−87%)
DMSO	13	18	2.3 (−9%)	6.1 (−91%)	18 (16%)	13
benzonitrile	5.2	14.8	3.8 (−35%)	13 (−65%)	14.8 (65%)	7

[a] Relative amplitudes are shown in parentheses for kinetics fitted by several exponentials [b] Should be assigned to excited-state solvation.

cations of nonradiative processes being dominant in the excited-state relaxation. Strong dependencies of the lifetimes on the solvent viscosity imply that some solvent-viscosity-controlled conformational reactions are responsible for the excited-state relaxation. The fluorescence yield increases significantly, and the excited-state lifetime extends up to several nanoseconds in a polymeric matrix, where such motion is hindered. Similar relaxation characteristics have been observed in numerous other large organic molecules and have usually been attributed to a barrierless excited-state isomerization.[19,20,27,28] The commonly accepted isomerization mechanism is thought to be a viscosity-controlled motion of the excited molecule along the conformational reaction coordinate toward the free energy minimum, where the energy gap between the excited and ground states is minimal. A subsequent fast nonradiative decay to the electronic ground state occurs from this conformation. Quantum chemical calculations indicate that such a process is possible for DMABI. The DMABI molecule has an excited-state free energy minimum at the twisted configuration. Thus, the excited-state twisting is a natural property of the excited molecule and the twisting angle should be considered as the main reaction parameter.

Another possible approach arises from the large difference between dipole moments of the DMABI molecule in the ground and excited states, indicating an intramolecular electron transfer. As was mentioned, reactions characterized by a solvent-aided stabilization of a charge-transfer state in a conformationally different configuration are attributed to a "TICT" type reaction. However, as will be shown later, the commonly used TICT concept is not completely adequate for the nonradiative excited-state relaxation taking place in the DMABI molecule.

Dynamic Fluorescence Shift. Solvation or Twisting? The excitation pulse creates population on the DMABI excited-state potential surface corresponding to the ground-state conformation, i.e., close to 0° of the twisting angle. According to the free energy scheme, population motion along the reaction coordinate−twisting angle should manifest itself as a dynamic red shift of the fluorescence band and as a decrease in the fluorescence intensity. The excited-state solvation should also induce a dynamical red shift of the fluorescence spectrum. Solvation dynamics is a highly nonexponential process, with fast (of the order of tens to hundreds of femtoseconds) and slow (on the order of a few to several tens of picoseconds) components in low- and medium-viscosity solvents,[74,75,80−85] i.e., proceeding on roughly the same time scale as the spectral evolution and the nonradiative relaxation processes observed in our experiments. The characteristic times of the dynamic fluorescence shifts of DMABI in DMSO, ethanol, and toluene are very close to the solvation dynamics observed for various other dye molecules in these solvents (see, for example, refs 74 and 75). The shift values are also typical of those of other molecules with similar ground- and excited-state static dipole moments in these solvents. Thus, the fluorescence spectral dynamics seems to be typical of solvation, while the influence of the molecular twisting is not clear. Moreover, since molecular twisting reduces the fluorescence oscillator strength, one should expect a fast fluorescence intensity decay during the fluorescence shift time if the shift is caused by molecular twisting. However, the absence of a fast component in the fluorescence decay with the same time constant as the Stokes shift dynamics indicates that the molecular twisting contributes little to the observed spectral shift. The two processes take place independently.

We compared the relative fluorescence quantum yields of DMABI in different solvents. The quantum yield is roughly proportional to the fluorescence lifetime, and this proportionality is valid even when the DMABI molecules are in a polymer matrix. This is an indication that the fluorescence oscillator strengths in all solvents and in a polymer matrix are equal. Since excited-state twisting in a polymer matrix is hardly possible (molecules are always flat), this fact is an additional indication that the fluorescence originates mainly from the flat molecular configuration. The same deduction may also be obtained from the analysis of the transient absorption spectra of the DMSO solution, showing that the stimulated emission oscillator strength is equal to that of the ground-state absorption. The arguments presented above imply that the DMABI fluorescence originates mainly from the nontwisted configuration and that the dynamic fluorescence shift is caused mainly by solvation.

Evidence for Molecular Twisting. Since the main properties of the fluorescence spectra dynamics may be explained by solvation, uninfluenced by the population dynamics along the twisting coordinate, a question that naturally arises is whether the fast nonradiative decay observed for DMABI in solution is really a consequence of twisting or if it is caused by the vibrational flexibility of the molecule. Such flexibility probably could also cause a viscosity dependence of the relaxation rate due to the solvent damping of vibrational motion. There are several arguments for twisting. Damping of vibrational motion in the polymeric matrix and in solvents can hardly be so different to cause the 3 orders of magnitude difference in the excited-state lifetimes. However, a strong difference may be expected if the fast nonradiative relaxation of the excited state is caused by the large-amplitude conformational changes, which are not possible in the polymer. The nonexponential fluorescence decay observed in the polymer is also in line with this model. Molecules with slightly twisted conformations or having some free space for twisting have shorter excited-state lifetimes, causing an inhomogeneous relaxation.

An unusually red-shifted fluorescence tail of DMABI in solution and the delay in appearance of this red fluorescence shoulder as observed in the time-resolved spectra are additional arguments for twisting taking place after excitation. Despite our conclusion that the fluorescence mainly originates from the nontwisted configuration and that the red shift is mainly caused by solvation, the weak red-shifted fluorescence may be attributed to various twisted configurations during the twisting process.

The transient absorption spectra and their time evolution reflect the dynamics of both the excited and ground states. The difference in relaxation times of the absorption bleaching and

stimulated emission is the strongest additional argument supporting the twisting reaction scheme. It may be interpreted by assuming that in the course of relaxation the DMABI molecules spend some time in a twisted "dark" state,[29,40,47] which may be characterized by zero (or low) absorption and stimulated emission cross sections.

Twisting Mechanism and Dynamics. Three possibilities for the excited-state twisting of the DMABI molecule can be suggested: (i) twisting of the dimethylamino group, (ii) twisting of the central single bond, or (iii) twisting of the central double bond. Twisting of the dimethylamino group usually results in relatively long-lived TICT states, resulting in the observation of a double fluorescence.[40] A considerable barrier is usually present for twisting of the dimethylamino group, resulting in the twisting rate being dependent on the solvent polarity. However, no double fluorescence was observed for DMABI and the excited-state reaction seems to be rather insensitive to the solvent polarity. Spectroscopic consequences of the twisting of the DMABI molecule are more similar to those of the nonradiative excited-state relaxation of triphenylmethane (TPM) molecules,[19] or 1,1′-diethyl-4,4′cyanine (1144-C) molecules,[27,28] where twisting of a C−C bond connecting two large molecular moieties takes place. These molecules also have a free energy minimum at 90° twisting angle in the excited state and a maximum in the ground state (the "sink" region);[17] this gives a small energy gap, which causes a fast internal conversion.

According to our quantum chemical calculations, only the central double bond twisting of DMABI results in a minimum of the excited-state potential energy, indicating that only this twisting reaction is energetically profitable (see Figure 2). This assignment is in agreement with the conclusion of Rettig[40] stating that the double bond twisting results in a very fast excited-state relaxation, while the single bond twisting usually creates relatively long-lived excited states and often results in a double fluorescence. Double bond twisting results in biradicaloid charge-transfer states (BCT),[40,41] which are usually characterized by a very short lifetime. Thus, these are the arguments that the central double bond twisting of the DMABI molecule takes place in the excited state.

Excited nπ^* states probably play an important role in the twisting reaction of DMABI molecules. According to our calculations the nπ^* states are lower in energy than the $\pi\pi^*$ state (see Figure 2). Fast relaxation from the $\pi\pi^*$ state to the nπ^* state would cause a fast fluorescence decay. However, such an electronic relaxation mechanism is in contradiction with the long fluorescence decay time, several nanoseconds, of DMABI in a polymer matrix. Two possible explanations for this disagreement can be suggested. First, our calculations neglect intermolecular interactions, which can change the relative energy positions of the two states. According to the general empirical rule, intermolecular interactions result in a decrease in energy of excited $\pi\pi^*$ states with respect to the energy of nπ^* states. Thus, an interchange of the nπ^* and $\pi\pi^*$ states is possible, resulting in the $\pi\pi^*$ state becoming the lowest excited state. In such a case, the diabatic potential energy curves of these two states must intersect at some twisting angle. According to an adiabatic approach, the intersection of the two potential energy curves is avoided at this point, which is usually described by assuming a mixing of the two states in the crossing region, reflecting the gradual transition from one electronic state to another. Another possible explanation is based on the assumption that the nπ^* and $\pi\pi^*$ states in a planar molecular conformation are very weakly coupled; therefore, a nonradiative transition between the two states is possible only when large conformational changes take place, which are not possible in the polymer matrix. Transition between the two states is probably much faster at the twisting angle (see Figure 2) where, according to our calculations, the optical transition between the ground and the first nπ^* state also gains in oscillator strength. Thus, in both cases transition to the nπ^* state occurs at some twisting angle, causing a fast subsequent molecular twisting toward a 90° configuration. The limiting stage of the DMABI twisting reaction is probably the diffusion-driven population motion on the flat potential energy maximum of the $\pi\pi^*$ state. At larger twisting angles, the molecular motion is determined by the slope of the nπ^* state potential energy and is much faster. Therefore, the population is never concentrated in this region of the twisting coordinate. The experimental data imply that the excited-state free energy dependence on the twisting coordinate of the DMABI molecules (Figure 15), with a flat maximum at a zero angle and minimum at 90°, is similar to that of stilbene.[29] However, the excited-state dynamics can be significantly different owing to the important influence of solvation dynamics as described above.

Excited-State Decay Rate. The time that the DMABI molecules spend in the "dark" state can be roughly estimated by comparing the decay times of the fluorescence and the absorption bleaching. For example, in the DMSO solution, where the fluorescence and absorption bleaching decay times are 13 and 18 ps, respectively, one can estimate that molecules spend about 5 ps in a "dark" state. This estimation is of course very rough, since the fluorescence transition dipole moment gradually decreases when the sink region is approached and the absorption dipole moment gradually increases when the ground state molecule comes back to the flat conformation. Thus, this time accounts for the excited-state lifetime in the sink region as well as the reduced transition dipole moment in the course of the twisting motion in the excited and ground states. There is even no evidence that the molecules reach the sink region. Probably the excited-state relaxation rate increases significantly already in the course of twisting, and the main part of the excited-state population relaxes to the ground state before actually reaching the sink region. In addition to the energy gap law[86] there are other possible factors leading to very fast nonradiative decay. Fast molecular conformational changes during the twisting motion might be one of such factors. The twisting motion is strongly coupled with various vibrational modes; therefore, molecular twisting induces shifts in the vibrational frequencies and shifts in the equilibrium positions of the atoms. Strong anharmonicity of the molecular vibrations increases the overlap of the ground- and excited-state vibrational modes, and consequently, a fast nonradiative relaxation rate can be caused by fast changes in molecular parameters. The decay rate due to this factor would depend on the twisting rate of the molecule rather than on the twist angle.

Ground-State Equilibration. Molecular relaxation in the ground state is the last stage of the twisting reaction. After the $S_1 \rightarrow S_0$ internal conversion, the molecule is still in a twisted geometry, which now corresponds to an out-of-equilibrium configuration. The system finds itself in a nonequilibrium state also with regard to the solvation coordinate, since this was relaxed to the stronger static dipole moment of the excited molecule. Moreover, the molecule contains a considerable amount of excess vibrational energy. All these aspects result in a nonstationary ground state with higher energy and consequently in a red shifted absorption spectrum, which expresses itself as a bleaching on the blue side of the absorption band and as an induced absorption on the red side. Thus, the induced absorption observed at 540 nm should be attributed to the

molecules in the nonequilibrium ground state. However, the absorption shift due to the ground-state equilibration should have practically no influence on the absorption bleaching measured close to the maximum of the absorption band at 490 nm. Monoexponental bleaching decay shows that the shift effect is really negligible. Therefore, the bleaching decay correctly reflects the ground-state recovery. Dynamics of the nonequilibrium ground-state population n_0^* may be approximately described by a relaxation of a three-level system $n_1 \rightarrow n_0^* \rightarrow n_0$. The rate equation for n_0^* is

$$dn_0^*/dt = k^* n_1 - k_{eq} n_0^* = k^* n_{1(t=0)} e^{-k^* t} - k_{eq} n_0^* \quad (8)$$

where the first term on the right-hand side expresses the increase in the population of the nonequilibrium ground state via $S_1 \rightarrow S_0$ internal conversion and the second one expresses the depopulation due to ground-state equilibration. The initial concentration of the excited molecules is represented by $n_{1(t=0)}$. The excited-state and nonequilibrium ground-state relaxation rates are k^* and k_{eq}, respectively. The solution of eq 8 is

$$n_0^* = \frac{k^* n_{1(t=0)}}{k^* - k_{eq}} (e^{-k_{eq} t} - e^{-k^* t}) \quad (9)$$

According to eq 9, the rise dynamics of the nonequilibrium ground-state population is always determined by the faster of the two relaxation rates, while the depopulation is determined by the slower one. It is important to keep in mind that qualitatively the n_0^* dynamics is the same whether $k_{eq} > k^*$ or $k_{eq} < k^*$. The situation may appear surprising when $k_{eq} > k^*$, since the rise dynamics of the nonequilibrium ground-state population is then determined by the equilibration rate k_{eq} while the decay dynamics is determined by the population rate k^*.

The transient absorption kinetics at 540 nm is complex (Figures 12 and 14). The signal can be separated into negative and positive contributions. At early times the signal is dominated by the ground-state bleaching and stimulated emission. At longer times, the positive contribution due to the nonequilibrium ground-state absorption becomes dominating. Since the bleaching appears instantaneously, the time evolution was fitted by a sum of three exponentials. The fastest component, τ^1_{540}, describing the decay of the negative signal, was found to be very close to the fluorescence shift time; thus, it corresponds to the red shift of the stimulated emission band and can be attributed to solvation dynamics. The two slower components τ^2_{540} and τ^3_{540} characterize the rise and decay of the nonequilibrium ground-state population. The decay time of the induced absorption, τ^3_{540}, was found to be close to the decay time of the absorption bleaching, τ_{490}, and in order to improve the stability of fitting, τ^3_{540} was fixed to the latter value. The arguments for identification of the two slower characteristic times with the relaxation processes are as follows. Molecules returning to the electronic ground state are initially out of equilibrium; thus, the population dynamics of the nonequilibrium ground state should be characterized by the same rate constant as the ground-state recovery. Since τ^3_{540} is equal to τ_{490}, this time constant may be attributed to the population of the nonequilibrium ground state. On the other hand, the time constant τ^2_{540}, which is always shorter than τ^3_{540}, characterizes the decay rate of the nonequilibrium ground state. We identify $k_{eq} = 1/\tau^2_{540}$. Thus, the unusual situation mentioned above occurs, where $k_{eq} > k^*$; i.e., the decay dynamics of the nonequilibrium ground state is determined by its population rate k^* and the rise dynamics is determined by the equilibration rate k_{eq}.

Transient absorption dynamics at 540 nm in different alcohols (see Figure 14) demonstrates another important feature of the induced absorption. The induced absorption is strong in the low-viscosity alcohol methanol, while it becomes much weaker in higher-viscosity propanol and is absent in decanol. A similar viscosity effect is observed in other solvents. If we identify the red-shifted ground-state absorption with a twisted ground-state configuration, the dependence of the induced absorption intensity on the solvent viscosity may be explained as follows. The rate of the excited-state nonradiative relaxation to the ground state increases gradually with the twisting angle. In the low-viscosity solvents the excited-state twisting is very fast, much faster than the $S_1 \rightarrow S_0$ internal conversion. Therefore, relaxation occurs when the twisting is over, and the resulting nonequilibrium ground-state population displays a high degree of twist. In high-viscosity solvents the excited-state twisting is much slower and the $S_1 \rightarrow S_0$ internal conversion takes place already during the twisting process, creating a nonequilibrium ground-state population that is less twisted. As a consequence, the corresponding transient absorption is less red-shifted.

It is worth noting that the ground-state equilibration k_{eq} is supposedly faster than the corresponding process in the excited state. The reason for this may be the absence of a barrier in the ground state, while in the excited state a low barrier may be present as indicated in the quantum chemistry calculations.

Two other aspects of the nonequilibrium ground-state mentioned above, solvation and molecular heating,[87] are probably not so important. Ground-state solvation should have approximately the same rate as that of the excited state, which is much faster than the induced absorption dynamics. Local heating of the nonequilibrium ground-state population would also explain the strong dependence of the induced absorption intensity on the solvent viscosity. The heated molecules are accumulated in solvents of low viscosity, where $S_1 \rightarrow S_0$ internal conversion is fast, while in solvents of high viscosity, where the internal conversion is slower, nonequilibrium molecules are distributed in time, and their concentration and consequently the red absorption shift is not substantial. However, cooling times of molecules in solution can hardly depend so strongly on the solvent viscosity, as is in the case of the methanol and propanol solutions where these times are 2.6 and 9.8 ps, respectively.

Charge-Transfer Dynamics. The influence of the solvent polarity on the DMABI twisting reaction is different from TICT reactions where usually a strong increase in the reaction rate with increasing solvent polarity is observed, the reaction often being absent in nonpolar solvents. The generally accepted TICT reaction model assumes that a locally excited (LE) state is created by optical excitation and that an intramolecular charge transfer subsequently takes place simultaneously with molecular twisting. Solvent polarity changes the free energy of the twisted state and consequently the TICT reaction dynamics. Twisting of DMABI takes place both in polar and in nonpolar solvents, and no strong influence of solvent polarity on the reaction dynamics is observed. There is even a tendency of the relaxation rate to decrease in highly polar solvents. This indicates that solvent polarity makes no strong influence on the energy difference between planar and twisted excited-state conformations. This is supported by the gas-phase quantum mechanical calculations, which show that no significant change in the molecule dipole moment occurs during the molecular twisting. Contrary to the typical TICT reaction, intramolecular charge transfer in DMABI is produced directly by optical transition. Even if the absorption involves a higher-lying LE state, a lower energy charge transfer (CT) state would be rapidly occupied via ultrafast excited-state

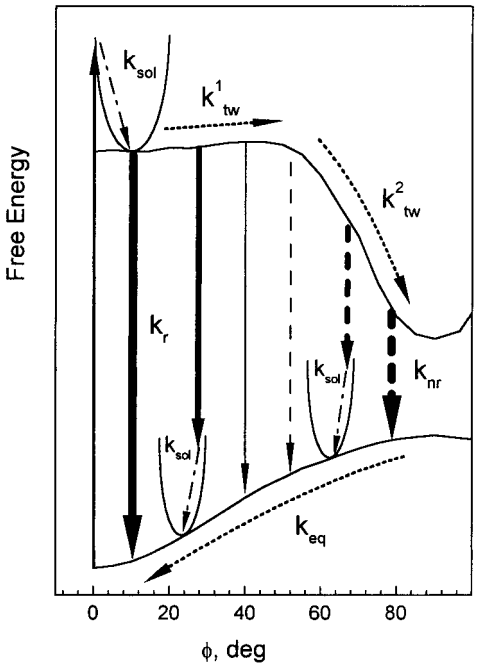

Figure 15. DMABI relaxation scheme. k_{sol} is the solvation rate, k^1_{tw} is the rate of diffusional twisting on a flat top of potential surface, k^2_{tw} is the twisting rate on the slope of potential surface, k_{nr} is the rate constant of the $S_1 \rightarrow S_0$ internal conversion, and k_{eq} is the ground-state equilibration rate. The thickness of the lines indicates the rate of the indicated processes.

internal conversion. Owing to the strong excited-state dipole moment, the solvent polarity significantly influences the absorption and fluorescence spectra by changing the energies of the solvated excited and ground states. However, since no significant charge redistribution takes place during the molecular twisting, no strong solvation influence on the twisting reaction dynamics is observed. A small reduction in the reaction rate with increasing solvent polarity mentioned above is probably not related to the changes of the potential surfaces but is caused by damping of molecular motion by the solvation shell. Thus, the DMABI excited-state reaction can hardly be assigned to a TICT reaction. The notation "charge-transfer-induced excited-state twisting" would be a more precise definition.

Relaxation Scheme. The schematic DMABI relaxation picture summarizing the results from our investigations is presented in Figure 15. The rate constants of the processes indicated in the scheme are as follows: k_{sol} is the solvation rate; k^1_{tw} is the rate of diffusional twisting on the flat top of the potential surface; k^2_{tw} is the twisting rate on the slope of the potential surface; k_{nr} is the rate constant of the $S_1 \rightarrow S_0$ internal conversion; k_{eq} is the ground-state equilibration rate.

According to the previous discussion, the rate constants are related approximately to the various observed fluorescence and transient absorption time constants by

$$1/k_{sol} \approx \tau_{shift} \approx \tau^1_{540}$$

$$1/k^1_{tw} \approx \tau_{fl} \approx \tau_{440} \approx \tau_{600}$$

$$1/k_{eq} \approx \tau^2_{540}$$

The excited-state lifetime approximately equals the sum of twisting and $S_1 \rightarrow S_0$ internal conversion times; thus, the excited-state decay rate k^* is approximately related to the other rate constants and experimental observables as

$$1/k^* \approx 1/k^1_{tw} + 1/k^2_{tw} + 1/k_{nr} \approx \tau^3_{540} \approx \tau_{490}$$

However, these relations should be seen as approximate only, since all the processes have similar rates and take place simultaneously. A quantitative separation and correct characterization would be a very complicated task. Moreover, most of the processes are nonexponential; thus, their characterization by rate constants is not completely correct.

Conclusions

Time-resolved picosecond transient absorption and femtosecond fluorescence spectroscopy were used for investigation of the excited-state relaxation of DMABI in solution and in the polymeric matrix. The central double bond twisting of the molecule was found to be responsible for the fast nonradiative excited-state deactivation. Different relaxation processes of DMABI in the excited and ground states were distinguished: excited-state solvation, population diffusion on the top of the excited-state potential surface, population drift on the slope of the excited-state potential surface, $S_1 \rightarrow S_0$ internal conversion, and finally, ground-state equilibration. The overall S_1 deactivation rate decreases by increasing the solvent viscosity; however, the viscosity dependence at various stages differs from each other. Despite the strong dipole moments of DMABI in both the ground and excited states, the solvent polarity has no strong influence on the reaction dynamics, but it significantly influences the absorption and fluorescence spectra and consequently the appearance of the transient absorption spectra. The main part of the fluorescence originates from the untwisted molecular configuration, and its spectral evolution is determined mainly by the excited-state solvation. On this time scale the population dynamics along the twisting coordinate has only a minor influence on the fluorescence spectra, but it determines the radiative and nonradiative excited-state relaxation rates. The charge-transfer-induced twisting rate is determined mainly by the diffusion-like population motion on the top of the excited-state potential energy surface, while the subsequent population drift on the slope of the potential surface and the nonradiative decay in the sink region ($S_1 \rightarrow S_0$ internal conversion) are much faster. Ground-state equilibration, which was identified as a back twisting of the DMABI molecule, completes the reaction. Twisted ground-state molecules more clearly express themselves in low-viscosity solvents where stronger excited-state twisting occurs before relaxation to the ground state.

The noninfluence of solvent polarity on the twisting reaction dynamics leads us to believe that the DMABI excited-state relaxation should be viewed as a "charge-transfer-induced excited-state twisting" rather than as a TICT reaction.

The twisting reaction identified in DMABI is hardly an exceptional case. Similar reactions probably occur in many other molecules previously attributed to form the TICT states. The relative positioning of the Franck−Condon LE and CT states is the main parameter determining which of the TICT or charge-transfer-induced twisting reaction takes place. If the Franck−Condon CT state has lower energy than the LE state, then charge transfer occurs directly by optical excitation or in the course of the ultrafast internal conversion, and the subsequent twisting process may be similar to that of DMABI.

Acknowledgment. This research was supported by the Lithuanian State Foundation of Science and Studies Grant No.291. We also thank Lithuanian Co. EKSMA for technical support.

References and Notes

(1) Wang, Y.; Crawfort, M. C.; Eisenthal, K. B. *J. Am. Chem. Soc*. **1982**, *104*, 5875.
(2) Bagchi, B.; Fleming, G. R. *J. Phys. Chem*. **1990**, *94*, 9.
(3) Sundström, V.; Aberg, U. *J. Mol. Liq*. **1993**, *57*, 149.
(4) Duxbury, D. F. *Chem. Rev*. **1993**, *93*, 381.
(5) Garavelli, M.; Celani, P.; Bernardi, F.; Robb, M. A.; Olivucci, M. *J. Am. Chem. Soc*. **1997**, *119*, 6891.
(6) Kosower, E. M. *J. Am. Chem. Soc*. **1985**, *107*, 1114.
(7) Sumi, H.; Marcus, R. A. *J. Chem. Phys*. **1986**, *84*, 4894.
(8) Huppert, D.; Ittah, V.; Kosower, E. M. *Chem. Phys. Lett*. **1988**, *144*, 15.
(9) Heitele, H.; Pollinger, F.; Weeren, S.; Michel-Beyerle, M. E. *Chem. Phys*. **1990**, *143*, 325.
(10) Weaver, M. J. *Chem. Rev*. **1992**, *92*, 463.
(11) Heitele, H. *Angew. Chem., Int. Ed. Engl*. **1993**, *32*, 359.
(12) Wynne, K.; Galli, C.; Hochstrasser, R. M. *J. Chem. Phys*. **1994**, *100*, 4797.
(13) Nagasawa, Y.; Yartsev, A. P.; Tominaga, K.; Bisht, P. B.; Johnson, A. E.; Yoshihara, K. *J. Phys. Chem*. **1995**, *99*, 653.
(14) Kuciauskas, D.; Lin, S.; Seely, G. R.; Moore, A. L.; Moore, T. A.; Gust, D.; Drovetskaya, T.; Reed, C. A.; Boyd, P. D. W. *J. Phys. Chem*. **1996**, *100*, 15926.
(15) Barbara, P. H.; Meyer, T. J.; Ratner, M. A. *J. Phys. Chem*. **1996**, *100*, 13148.
(16) Damrauer, N. H.; Cerullo, G.; Yeh, A.; Boussie, T. R.; Shank, Ch. V.; McCusker, J. K. *Science* **1997**, *275*, 54.
(17) Bagchi, B.; Fleming, G. R.; Oxtoby, D. W. *J. Chem. Phys.* **1983**, *78*, 7375.
(18) Dietz, F.; Rentsch, S. K. *Chem. Phys.* **1985**, *96*, 145.
(19) Ben-Amotz, D.; Harris, C. B. *Chem. Phys. Lett*. **1985**, *119*, 305.
(20) Åkesson, E.; Bergström, H.; Sundström, V.; Gillbro, T. *Chem. Phys. Lett*. **1986**, *126*, 385.
(21) Barbara, P. F.; Jarzeba, W. *Acc. Chem. Res*. **1988**, *21*, 195.
(22) Bagchi, B.; Åberg, U.; Sundström, V. *Chem. Phys. Lett*. **1989**, *162*, 227.
(23) Åberg, U.; Sundström, V. *Chem. Phys. Lett*. **1991**, *185*, 461.
(24) Korppi-Tommola, J. E. I.; Hakkarainen, A.; Hukka, T.; Subbi, J. *J. Phys. Chem*. **1991**, *95*, 8482.
(25) Åkesson, E.; Hakkarainen, A.; Laitinen, E.; Helenius, V.; Gillbro, T.; Korppi-Tommola, J.; Sundström, V. *J. Chem. Phys*. **1991**, *95*, 6508.
(26) Waldeck, D. H. *J. Mol. Liq*. **1993**, *57*, 127.
(27) Åberg, U.; Åkesson, E.; Fedchenia, I.; Sundström, V. *Isr. J. Chem.* **1993**, *33*, 167.
(28) Åberg, U.; Åkesson, E.; Alvarez, J.-L.; Fedchenia, I.; Sundström, V. *Chem. Phys*. **1994**, *183*, 269.
(29) Vachev, V. D.; Frederick, J. H.; Grishanin, B. A.; Zadkov, V. M.; Koroteev, N. I. *J. Phys. Chem.* **1995**, *99*, 5247.
(30) Stock, G. *J. Chem. Phys*. **1995**, *103*, 10015.
(31) Harju, T. O.; Korppi-Tommola, J. E. I.; Huizer, A. H.; Varma, C. A. G. O. *J. Phys. Chem*. **1996**, *100*, 3592.
(32) Pullen, H.; Anderson, N. A.; Walker, L. A., II; Sension, R. J. *J. Chem. Phys*. **1997**, *107*, 4985.
(33) Rotkiewicz, K.; Grellman, K. H.; Grabowski, Z. R. *Chem. Phys. Lett*. **1973**, *19*, 315.
(34) Rotkiewicz, K.; Rubaszewska, W. *Chem. Phys. Lett*. **1980**, *70*, 444.
(35) Huppert, D.; Rand, S. D.; Rentzepis, P. M.; Barbara, P. F.; Struve, W. S.; Grabowski, Z. R. J. *Chem. Phys*. **1981**, *75*, 5714.
(36) Wang, Y.; Eisenthal, K. B. *J. Chem. Phys*. **1982**, *77*, 6076.
(37) Rettig, W. *J. Phys. Chem*. **1982**, *86*, 1970.
(38) Grabowski, Z. R.; Dobkowski, J. *Pure Appl. Chem*. **1983**, *55*, 245.
(39) Rettig, W. *Angew. Chem., Int. Ed. Engl*. **1986**, *25*, 971.
(40) Rettig, W. In *Topics of Current Chemistry*; Springer-Verlag: Berlin, 1994; p 254.
(41) Lippert, E.; Rettig, W.; Bonačić-Koutecký, V.; Heisel, F.; Miehe, J. A. *Adv. Chem. Phys*. **1987**, *68*, 1.
(42) Momicchioli, F.; Baraldi, I.; Berthier, G. *Chem. Phys*. **1988**, *123*, 103.
(43) Herbich, J.; Salgado, F. P.; Rettschnick, R. P. H. Grabowski, Z. R.; Wojtowicz, H. *J. Phys. Chem*. **1991**, *95*, 3491.
(44) Rettig, W.; Baumann, W. In *Photochemistry and Photophysics*; Rabek, J. F., Ed.; CRC Press: Boca Raton, FL, 1992; Vol. 6, p 79.
(45) Bhattacharyya, K.; Chowdhury, M. *Chem. Rev*. **1993**, *93*, 507.
(46) Sun, Y.-P.; Bowen, T. L.; Bunker, C. E. *J. Phys. Chem*. **1994**, *98*, 12486.
(47) Markovitsi, D.; Sigal, H.; Ecoffet, C.; Millie, P.; Charra, F.; Fiorini, C.; Nunzi, J.-M.; Strzelecka, H.; Veber, M.; Jallabert, C. *Chem. Phys*. **1994**, *182*, 69.
(48) Sato, Y.; Morimoto, M.; Segawa, H.; Shimidzu, T. *J. Phys. Chem*. **1995**, *99*, 35.
(49) Soujanya, T.; Saroja, G.; Samanta, A. *Chem. Phys. Lett*. **1995**, *236*, 503.
(50) Hayashi, S.; Ando, K.; Kato, S. *J. Phys. Chem*. **1995**, *99*, 955.
(51) Catalan, J.; D'az, C.; Lopez, V.; Perez, P.; Claramunt, R. M. *J. Phys. Chem*. **1996**, *100*, 18392.
(52) Kohler, G.; Rechthaler, K.; Rotkiewicz, K.; Rettig, W. *Chem. Phys*. **1996**, *207*, 85.
(53) Kim, H. J.; Hynes, J. T. *J. Photochem. Photobiol*. **1997**, *105*, 337.
(54) Albinsson, B. *J. Am. Chem. Soc*. **1997**, *119*, 6369.
(55) Warren, J. A.; Bernstein, E. R.; Seeman, J. I. *J. Chem. Phys*. **1988**, *88*, 871.
(56) Weisenborn, P. C. M.; Huizer, H.; Varma, C. A. G. O. *Chem. Phys.* **1989**, *133*, 437.
(57) Grassian, V. H.; Warren, J. A.; Bernstein, E. R.; Secor, H. V. *J. Chem. Phys*. **1989**, *90*, 3994.
(58) Shang, Q.; Bernstein, E. R. *J. Chem. Phys*. **1992**, *97*, 60.
(59) Hebert, P.; Baldacchino, G.; Gustavsson, T.; Mialocq, J.-C. *Chem. Phys. Lett*. **1993**, *213*, 345.
(60) Hebert, P.; Baldacchino, G.; Gustavsson, T.; Mialocq, J.-C. *J. Photochem. Photobiol*. **1994**, *84*, 45.
(61) Martin, M. M.; Plaza, P.; Meyer, Y. H. *Chem. Phys*. **1995**, *192*, 367.
(62) Zachariasse, K. A.; Grobys, M.; Haar, T.; Hebecker, A.; Il'ichev, Y. V.; Jiang, Y.-B.; Morawski, O.; Kuhnle, W. *J. Photochem. Photobiol.* **1996**, *102*, 59.
(63) Kovalenko, S. A.; Ernsting, N. P.; Ruthmann, *J. Chem. Phys*. **1997**, *106*, 3504.
(64) Lippert, E.; Luder, W.; Boos, H. In *Advances in Molecular Spectroscopy*; Mangini, A., Ed.; Pergamon: Oxford, 1962; p 443.
(65) Agranat, I.; Loewenstein, R. M. J.; Bergmann, E. D. *Isr. J. Chem*. **1969**, *52*, 89. Dimond, N. A.; Mukherjee, T. K. *Discuss. Faraday. Soc*. **1971**, *51*, 102.
(66) Magomedova, N. S.; Zvonkova, Z. V. *Kristallografiya* **1978**, *23*, 281 (in Russian).
(67) Valkunas, L.; Juodzbalis, D.; Urbas, A.; Gruodis, A.; Durandin, A.; Silinsh, E. A.; Klimkans, A.; Larsson, S. *Adv. Mater. Opt. Electron*. **1993**, *2*, 221. Balevicius, M.; Stumbrys, E.; Sorokolit, B.; Gruodis, A. *Lithuanian J. Phys.* **1995**, *35*, 20.
(68) Volosov, A. *J. Chem. Phys.* **1987**, *87*, 6653.
(69) Frisch, M. J.; Trucks, G. W.; Schlegel, H. B.; Gill, P. M. W.; Johnson, B. G.; Robb, M. A.; Cheeseman, J. R.; Keith, T.; Petersson, G. A.; Montgomery, J. A.; Raghavachari, K.; Al-Laham, M. A.; Zakrzewski, V. G.; Ortiz, J. V.; Foresman, J. B.; Cioslowski, J.; Stefanov, B. B.; Nanayakkara, A.; Challacombe, M.; Peng, C. Y.; Ayala, P. Y.; Chen, W.; Wong, M. W.; Andres, J. L.; Replogle, E. S.; Gomperts, R.; Martin, R. L.; Fox, D. J.; Binkley, J. S.; Defrees, D. J.; Baker, J.; Stewart, J. P.; Head-Gordon, M.; Gonzalez, C.; Pople, J. A. *Gaussian 94*, revision D2; Gaussian Inc.: Pittsburgh, PA, 1995.
(70) Becke, A. D. *J. Chem Phys.* **1993**, *98*, 5648.
(71) Michl, J.; Bonačić-Koutecký, V. *Electronic Aspects of Organic Photochemistry*; John Wiley & Sons: New York, 1990.
(72) Aleksandrov, S. B.; Meiyere, G. F.; Yurel, S. P. *Organic Semiconductor Materials*, 3rd ed.; Perm University, Russia, 1980; Chapter 1 (in Russian).
(73) Gustavsson, T.; Baldacchino, G.; Mialocq, J.-C.; Pommeret, S. *Chem. Phys. Lett*. **1995**, *236*, 587.
(74) Edward, W.; Castner, J.; Maroncelli, M.; Fleming, G. R. *J. Chem. Phys.* **1987**, *86*, 1090.
(75) Horng, M. L.; Gardecki, J. A.; Papazyan, A.; Maroncelli, M. *J. Phys. Chem*. **1995**, *99*, 17311.
(76) Kamlet, M. J.; Abboud, J. L.; Taft, R. W. *J. Am. Chem. Soc*. **1977**, *99*, 6027.
(77) Kamlet, M. J.; Dickinson, C.; Taft, R. W. *Chem. Phys. Lett*. **1981**, *77*, 69.
(78) Kamlet, M. J.; Abboud, J. L. M.; Abraham, M. H.; Taft, R. W. *J. Org. Chem.* **1983**, *48*, 2877
(79) Marcus, Y.; Kamlet, M. J.; Taft, R. W. *J. Phys. Chem.* **1988**, *92*, 3613.
(80) Martini, I.; Hartlant, G. V. *Chem. Phys. Lett*. **1996**, *258*, 180.
(81) Martini, I.; Hartlant, G. V. *J. Phys. Chem*. **1996**, *100*, 19764.
(82) Bingemann, D.; Ernsting, M. P. *J. Chem. Phys*. **1995**, *102*, 2691.
(83) Stratt, R. M.; Maroncelli, M. *J. Phys. Chem*. **1996**, *100*, 12981.
(84) Passino, S. A.; Nagasawa, Y.; Joo, T.; Fleming, G. R. *J. Phys. Chem. A* **1997**, *101*, 725.
(85) Rubtsov, I.; Yoshihara, K. *J. Phys. Chem. A* **1997**, *101*, 6138.
(86) Elsaesser, T.; Kaiser, W. *Annu. Rev. Phys. Chem*. **1991**, *42*, 83.
(87) Valkunas, L.; Gulbinas, V. *Photochem. Photobiol*. **1997**, *66*, 628.